Robotica (2014) volume 32, pp. 279–290. © Cambridge University Press 2014
doi:10.1017/S0263574714000113

Distributed amorphous ramp construction in unstructured environments

Nils Napp†* and Radhika Nagpal‡

†*Wyss Institute for Biologically Inspired Engineering, Harvard University, 33 Oxford Street, Cambridge, MA 02138, USA*
‡*School of Engineering and Applied Sciences, Harvard University, 33 Oxford Street, Cambridge, MA 02138, USA*

(Accepted January 6, 2014. First published online: February 26, 2014)

SUMMARY
We present a model of construction using iterative amorphous depositions and give a distributed algorithm to reliably build ramps in unstructured environments. The relatively simple local strategy for interacting with irregularly shaped, partially built structures gives rise to robust adaptive global properties. We illustrate the algorithm in both single robot and multi-robot cases via simulations and describe how to solve key technical challenges to implementing this algorithm via a robotic prototype.

KEYWORDS: Control of robotic systems; Bioinspired robots; Mobile robots; Multi-robot systems; Novel applications of robotics.

1. Introduction

Robots are best suited for dirty, dull, and dangerous tasks. This paper focuses on algorithms for the dirty and dangerous task of construction in unstructured terrain. Applications range from rapid disaster response, such as building levees and support structures, to remote construction in mines or space. The requirement of working in unstructured terrain frequently coincides with a lack of infrastructure, such as global positioning or a consistent shared global state estimate, which simplify coordination of multiple robots and deliberative planing. Distributed algorithms that use limited local information and coordinate through stigmergy solve this problem and provide scalable solutions. Robustness to poor sensing and irregular terrain can further be improved by using *amorphous* construction materials that comply with obstacles. Such construction is locally reactive on both an algorithmic level, i.e. where robots deposit based on local cues, and a physical level, i.e. amorphous construction materials react by changing shape to conform to their environment.

Our approach is inspired by biological systems, such as mound building termites,[20] that are very adept at building in unstructured terrain (Fig. 1(a)). Their skill combines scalable coordination through stigmergy and the use of amorphous building materials that interface with irregular environments. We would like to endow scalable robot teams with similar skill, however an algorithmic foundation for doing so is lacking. Current models for autonomous robotic construction focus on assembling pre-fabricated building materials and cannot accommodate the continuous nature of amorphous building materials. The contribution of this paper is two-fold: (a) A mathematical framework for reasoning about robots that construct with amorphous materials, and (b) a distributed, locally reactive algorithm for adaptive ramp building. This work is a step away from robots assembling discrete pre-fabricated components and instead embracing the messy continuous world (Fig. 1(b)).

Section 2 presents mathematical models for amorphous construction and adaptive ramp building. Section 3 gives a local strategy for creating structures that robots can climb. Section 4 extends those results to include physical constraints for single and multiple robots. Section 5 discusses future work.

* Corresponding author. E-mail: nnapp@wyss.harvard.edu

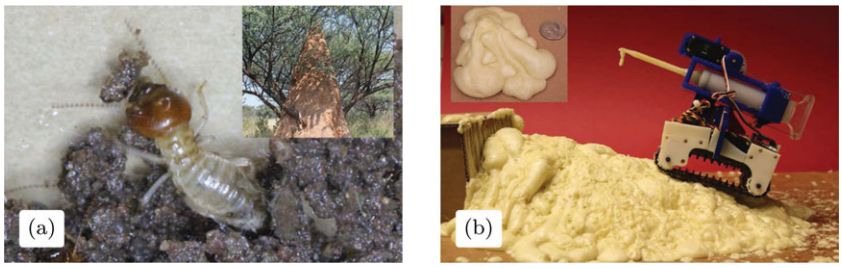

Fig. 1. (Colour online) Examples of amorphous construction. (a) Amorphous construction in biology. A termite preparing an amorphous dollop of mud for deposition. Inset shows a mound built around a tree. (b) Prototype of a construction robot. The robot was remote controlled to build a ramp using amorphous foam depositions. Inset shows a cone-shaped deposition.

1.1. Related work

Currently, there is much interest in the topic of robotic construction with mobile robots,[4,5,7,11,12,17] as well as decentralized algorithms by which multiple robots can coordinate construction.[1,10,13,19] These systems are mainly focused on building pre-specified structures using lattice-based building materials.[6,22] Lattice-based building blocks have good structural properties – being strong, stiff, and light – but place assumptions on the initial environment being level and devoid of obstacles. These methods are difficult to extend to unstructured environments with irregularly shaped obstacles. Furthermore, alignment and attachment restrictions affect all other aspects of design, for example, adding complex assembly order constraints.

In contrast, amorphous building materials – e.g. foam, mud, sandbags, or compliant blocks – sidestep these limitations.[14] They can help compensate for uncertainty and measurement errors without requiring complex sensing or reasoning. For example, compliant and amorphous materials are used for rapidly building flood protection in disaster zones[8,21] or pouring foundations over irregular terrain. Similarly, the requirement of fixed attachment orientations can be relaxed by using adhesive in the autonomous robotic construction of curved walls.[2,4] The closely related works[3,18] use amorphous materials, such as hot-melt adhesive or foam, to adapt robot parts to unknown tasks. Digital manufacturing via CAD/CAM, and some large-scale robotic construction systems, such as Contour Crafting,[9] also use amorphous materials to build continuous shapes. While these systems are not specifically focused on construction in unstructured environments, we can exploit the materials and design principles to design robots that utilize amorphous materials.

2. Problem Formulation and Questions

We present a solution to the *adaptive ramp building* problem as a particular example of a distributed construction task in unstructured terrain. The problem is to design a deposition and motion strategy to reach an arbitrary goal position despite irregularly shaped obstacles. Robots can sense the goal direction, move on partially built structures, and deposit amorphous materials to make non-climbable structures climbable. Adaptive ramp building is an example of how amorphous construction materials can be used to create robust behavior, and also provides a primitive behavior for solving more complex tasks. The remainder of this section presents mathematical models for continuous structures, amorphous depositions, and climbable structures.

2.1. Mathematical model for continuous structures

We model construction in two or three dimensions. Gravity constrains robots to move along surfaces on which they can incrementally deposit construction material. We assume that the *construction area* Q is a connected, compact, and finite subset of $\mathbb{R}^1$ (or $\mathbb{R}^2$) and the domain of a bounded, non-negative height function, $h : Q \to \mathbb{R}^+$. The graph of h, $(x, h(x))$ $x \in Q$, describes a *structure*. Robots move on structures and modify them.

If structures are modeled as functions, depositions are operators on functions. To distinguish the two, function spaces are denoted by scripted letters. For example, let $\mathcal{Q}$ be the space of real-valued, bounded functions on Q, and $\mathcal{Q}^+ \subset \mathcal{Q}$ is the subset of non-negative ones. Function application to points is denoted by parentheses $(\cdot)$, and operator application to functions is denoted by brackets $[\cdot]$.

https://doi.org/10.1017/S0263574714000113 Published online by Cambridge University Press

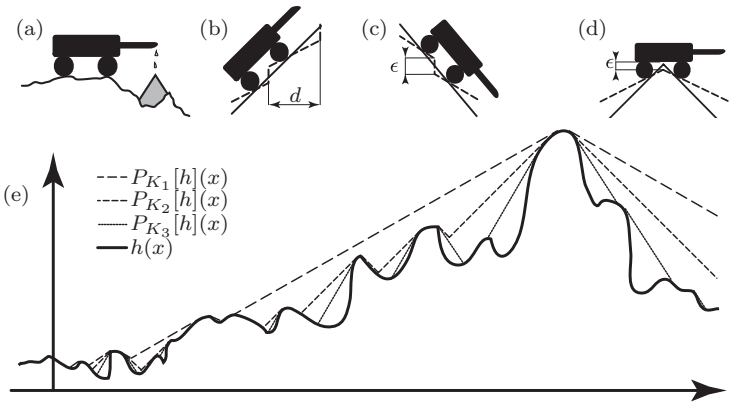

Fig. 2. Parameter geometry. (a) Robot making an amorphous deposition (gray). The top surface is defined by the deposition's shape function f. The bottom is defined by the environment h. (b) and (c) Relation of K to the maximal steepness a robot can climb and descend with (dashed) and without (solid) a discontinuity. (d) Relation of steepness K to the required ground clearance to drive over the apex of a cone. (e) A height function on h and its projections onto Lipschitz functions with different parameters, $K_3 > K_2 > K_1$.

For example, applying function $h \in \mathcal{Q}^+$ to a point $x \in Q$ is written as $h(x)$, and applying operator $D : \mathcal{Q}^+ \to \mathcal{Q}^+$ to h is denoted by $D[h]$. In the case of functions, all relational symbols should be interpreted pointwise, e.g. given $h, g \in \mathcal{Q}^+$, $h \leq g \equiv h(x) \leq g(x)\ \forall x \in Q$.

One limitation of modeling structures as functions is that many physical terrains have overhangs and are not functions. However, the benefit of this restrictive model is that it comes with analysis tools, such as continuity and integration, that can be used to reason about construction algorithms.

2.2. Model for amorphous deposition

Robots can deposit amorphous construction material and control its volume and position (Fig. 1(b)). The top surface of each deposition is modeled by a *shape function* $f \in \mathcal{Q}$, which the robot can control, while the bottom conforms to the structure (Fig. 2(a)). As a simple, yet sufficiently general, family of shape functions we use cones. Given an apex position $(\phi, \sigma) \in Q \times \mathbb{R}^+$ and steepness $K_D \in \mathbb{R}^+$, let

$$f_{(\phi,\sigma)}(x) = \sigma - K_D|\phi - x|. \tag{1}$$

The deposition operator $D : \mathcal{Q} \times \mathcal{Q}^+ \to \mathcal{Q}^+$ models interactions of depositions with the environment, here simply covering it. Given a structure $h \in \mathcal{Q}^+$ with $h(\phi) < \sigma$, the new structure after deposition $f_{(\phi,\sigma)}$ is given by

$$D[f_{(\phi,\sigma)}, h](x) = \max\{f(x), h(x)\}. \tag{2}$$

Given an initial structure $h_0 \in \mathcal{Q}^+$, larger structures are built up by a sequence of depositions, each characterized by their shape parameters (ϕ_1, σ_1), (ϕ_2, σ_2), (ϕ_3, σ_3), etc. The height function h_n after n depositions is defined recursively by

$$h_n(x) = D[f_{(\phi_n,\sigma_n)}, h_{n-1}](x). \tag{3}$$

After the nth deposition, the local reactive rules of each robot direct it to move on h_n and possibly make a deposition resulting in a new structure h_{n+1}.

This deposition model preserves continuity, independent of the particular parameter choices (ϕ_n, σ_n). In this and the following proofs, $B_\varepsilon(x)$ denotes the *open ball* of radius ε around x, i.e. $y \in B_\varepsilon(x)$ if and only if $|y - x| < \varepsilon$.

Lemma 1. *Given a continuous $h_0 \in \mathcal{Q}^+$ and $\varepsilon \in \mathbb{R}^+$, then $\exists \delta$ s.t. $\forall x \in Q$, $\forall y \in B_\delta(x)$, and any h_n created according to* (3)*, $h_n(y) \in B_\varepsilon(h_n(x))$.*

https://doi.org/10.1017/S0263574714000113 Published online by Cambridge University Press

Proof. By continuity of h_0 and compactness of Q, for any given $\varepsilon \in \mathbb{R}$ $\exists \delta'$ s.t. $\forall y \in B_{\delta'}(x)$, $h_0(y) \in B_\varepsilon(h(x))$. By construction of h_n, $\delta = \min\{\delta', \varepsilon/K_D\}$ has the above property. □

Our proposed solution to the ramp building problem can accommodate uncertainty in both deposition location and size, see end of Section 4.1. However, for clarity we assume an exact shape function f in the following presentation.

2.3. Navigable structures

Building a ramp means turning a structure that robots cannot climb into one they can climb. As such, any algorithm to adaptively build ramps needs a tractable description of climbable structures. This section defines the notion of *navigable* functions on Q, which represent climbable physical structures.

We use three parameters to describe robot-specific motion constraints: $K \in \mathbb{R}^+$, to model the maximum steepness robots can drive up or down, $\epsilon \in \mathbb{R}^+$, to model the largest discontinuity robots can freely move past, and $d \in \mathbb{R}^+$, to limit the amount of discontinuity in a small area (i.e. robot length) (Figs. 2(b)–(d)). Formally, navigable structures are locally (parameter d) close (parameter ϵ) to K-Lipschitz continuous (Naylor and Sell, p. 594),[16] i.e.

$$|h(x) - h(y)| \leq K|x - y| \; \forall x, y \in Q. \tag{4}$$

Specifically, function $h \in \mathcal{Q}$ is called navigable if and only if

$$|h(x) - h(y)| \leq \epsilon + K|x - y| \; \forall x, y \in Q \text{ and } |x - y| \leq d. \tag{5}$$

To reason about global guarantees of our local algorithms, we construct the operator P_K, defined by (7). It maps any structure to the *closest* K-Lipschitz function that can be built by only adding material, Fig. 2(e). At a given point, $x \in Q$, P_K takes the maximum value of any cones that need to be added, so all other points fulfill condition (4). There are two important properties of P_K. First, by construction

$$P_K[h](x) \geq h(x) \; \forall h \in \mathcal{Q}. \tag{6}$$

Since depositions are additive, it is important that $P_K[h]$ can be reached by only adding to h. Second, $P_K[h]$ returns the smallest function in $\mathcal{L}_K$, the space of K-Lipschitz functions on Q, in the following sense.

Theorem 2. *Given any two functions $h \in \mathcal{Q}$ and $g \in \mathcal{L}_K$ with $g \geq h$, the operator*

$$P_K[h](x) = \max_{y \in Q}\{h(y) - K|y - x|\} \tag{7}$$

with $K \in \mathbb{R}^+$, has the following properties:

1. *$P_K[h]$ is K-Lipschitz, and*
2. *$g \geq P_K[h]$.*

See Section 6 for proof. The following theorem shows that if steeper features are allowed, less material needs to be added (Fig. 2(d)).

Theorem 3. *Given an arbitrary function $h \in \mathcal{Q}$ and $K_1, K_2 \in \mathbb{R}^+$ with $K_1 \leq K_2$ the projections onto $\mathcal{L}_{K_1}$ and $\mathcal{L}_{K_2}$ obey $P_{K_2}[h] \leq P_{K_1}[h]$.*

Proof. For a given point $y \in Q$ in (7), $h(y) - K_2|y - x| \leq h(y) - K_1|y - x|$ since $|y - x|$ is non-negative.

□

Given an initial function h_0, the next section gives a locally reactive deposition strategy such that after N depositions h_N is navigable, i.e. fulfills (5), and is bounded above by $P_K[h_0]$.

https://doi.org/10.1017/S0263574714000113 Published online by Cambridge University Press

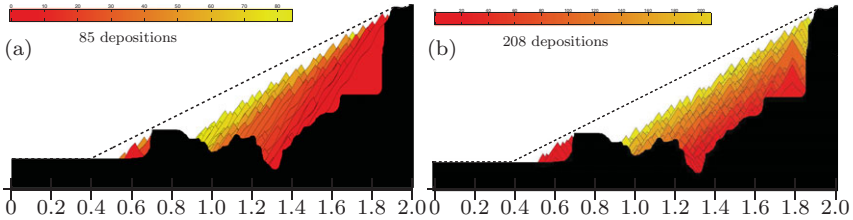

Fig. 3. (Colour online) Simulations of deposition algorithms. The initial structure h_0 is shown as solid black, and the upper bound $P_K[h_0]$ is shown as a dashed black line. The simulation parameters are: $Q = [0, 2]$, $K = 0.5$, $K_D = 1.5$, $\epsilon = 0.05$, and $d = 0.1$. Depositions progressively change colour, see colour-bar. (a) Deposition locations are picked randomly and their heights according to Algorithm 1. (b) Deposition locations and heights are picked according to Algorithm 2, with $x_0 = 0.2$ and $x_* = 1.9$. As the colours show, in both cases information about the cliff on the right propagates backwards through stigmergy. Additional motion and deposition height constraints in Algorithm 2 result in a layered structure and smaller depositions, see simulation movies.[15] The simulations incorporate additive noise to the deposition shape function, see Section 4.1.

Algorithm 1 Local deposition strategy. Pick point pairs that imply a local non-navigable feature and deposit on the lower one.

Given $h \in \mathcal{Q}^+$.
$h_0 \leftarrow h$
while $\exists\, x, y \in Q$ s.t. $|x - y| \leq d$, $K|y - x| + \epsilon < |h_n(y) - h_n(x)|$ **do**
  if $h_n(x) < h_n(y)$ **then**
    $x' \leftarrow x$
    $y' \leftarrow y$
  else
    $x' \leftarrow y$
    $y' \leftarrow x$
  end if
  Pick any $\omega \in [\epsilon, h_n(y') - h_n(x') - K|x' - y'|]$
  Deposit at x' with height ω, i.e. $h_{n+1} = D[f_{(x', \omega + h_n(x'))}, h_n]$
end while

3. Local Reactive Deposition Algorithm

In a *local* deposition strategy, robots with limited sensing range $r \in \mathbb{R}^+$ (with $r > d$) move on top of the structure and *react* to features in their sensing range. Algorithm 1 relates local checks and depositions to global properties. It checks for points that imply a non-navigable feature and deposits in such a way as to decrease the distance from the current structure to the closest K-Lipschitz structure. Specifically, Algorithm 1 searches for points $|y - x| \leq d$ s.t.

$$|y - x|K + \epsilon < |h(y) - h(x)|. \tag{8}$$

3.1. Correctness of local deposition strategy

The correct behavior of Algorithm 1 is that after a finite number of depositions the resulting structure h_N is navigable. The proof proceeds in two steps: (a) Theorem 4 shows progress, i.e. every deposition has a strictly positive volume. (b) Theorem 5 shows depositions obey the invariant upper bound $P_K[h_0]$. By combining them, Theorem 6 shows correct behavior. Note that since $P_K[h_0]$ is the smallest dominating K-Lipschitz function, Algorithm 1 is also efficient in the sense that it avoids unnecessary depositions, i.e. construction beyond the conservatively navigable $P_K[h_0]$ (Fig. 3(a)).

The *volume* of the difference between two structures g and $h \in \mathcal{Q}^+$ is given by

$$V(g, h) = ||g - h||_1 \equiv \int_Q |g(x) - h(x)|\, dx. \tag{9}$$

Similarly, the volume of a particular deposition is given by $V(D[f_{(\phi,\sigma)}, h], h)$.

https://doi.org/10.1017/S0263574714000113 Published online by Cambridge University Press

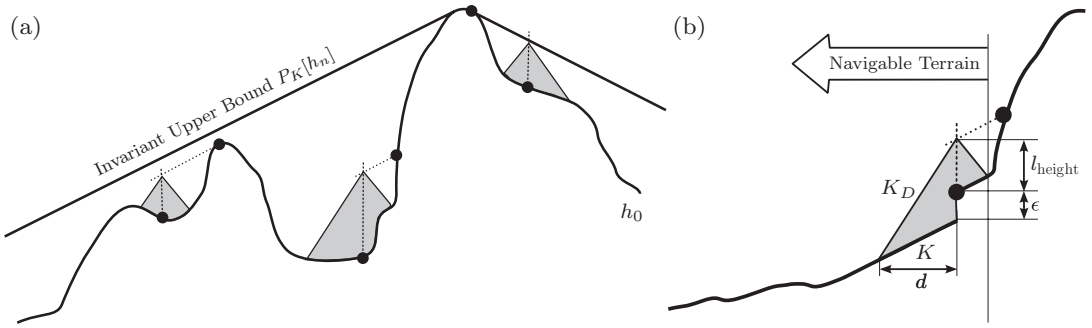

Fig. 4. Diagrams for proofs in Sections 3 and 4.(a) Diagram of Theorem 5. When point pairs and depositions are picked according to Algorithm 1, shown in gray, the mapping to $\mathcal{L}_K$ remains invariant, i.e. $P_K[h_n] = P_K[h_0]$. (b) Parameter constraints for Algorithm 2. When robot parameters shown in Fig. 5(a) fulfill condition (11), the maximum extent that a deposition can have into previously navigable terrain is limited by d.

Theorem 4 (Progress). *Given a pair of points $x, y \in Q$ s.t. $h_n(x) < h_n(y)$ and the property that*

$$|x - y|K + \epsilon < |h_n(x) - h_n(y)|,$$

depositing on x with a height

$$\omega \in \left[\epsilon, \frac{h_n(y) - h_n(x)}{K|x - y|}\right]$$

results in a deposition volume $V(D[f_{(x,\omega)}, h_n], h_n) > \varepsilon$ that is bounded below by a strictly positive number.

Proof. Note that the deposition height is at least ϵ. By Lemma 1, there exists some δ s.t. h_n maps every $B_\delta(x) \subset Q$ into $B_{\epsilon/3}(h_n(x))$. As a result, $\forall p \in B_\delta(x)$, $h(p) < h(x) + \frac{\epsilon}{3}$, and $h(x) + \frac{2\epsilon}{3} < D[f_{(x,\omega)}, h_n](p)$. Therefore, $V(D[f_{(x,\omega)}, h_n], h_n) > \int_{B_\delta(x)} \frac{\epsilon}{3} = \varepsilon > 0$. □

Theorem 5 (Invariant). *Assuming that $K_D > K$, depositions made with Algorithm 1 leave the mapping onto $\mathcal{L}_K invariant$, i.e. $P_K[h_n] = P_K[h_0]$.*

See Fig. 4(a) for an illustration and Section 6 for proof.

Theorem 6. *Given an initial structure $h_0 \in \mathcal{Q}^+$, following Algorithm 1 terminates after a finite number of steps, N; and for no points in Q does h_N fulfill non-navigability condition* (8)*, i.e. $\forall z \in Q$ and $x, y \in B_{\frac{d}{2}}(z)$,*

$$|x - y|K + \epsilon \geq |h_N(x) - h_N(y)|.$$

Proof. The expression for the remaining volume $V(P[h_0], h_n) = ||P[h_0] - h_n||_1 = \int_Q |P[h_0](x) - h_n(x)|dx$ can be rewritten as

$$\int_Q |P[h_0](x) - h_{n+1}(x) + h_{n+1}(x) - h_n(x)|dx.$$

By Theorems 5 and 6, $P[h_0](x) - h_{n+1}(x) \geq 0$ and $h_{n+1}(x) - h_n(x) \geq 0$, therefore

$$\begin{aligned} V(P[h_0], h_n) &= \int_Q |P[h_0](x) - h_{n+1}(x)|dx + \int_Q |h_{n+1}(x) - h_n(x)|dx \\ &= V(P[h_0], h_{n+1}) + V(h_{n+1}, h_n). \end{aligned}$$

https://doi.org/10.1017/S0263574714000113 Published online by Cambridge University Press

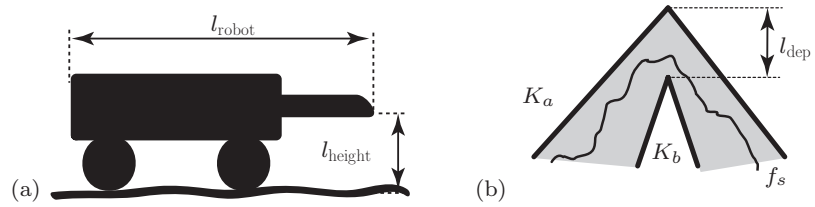

Fig. 5. Physical parameters. (a) Relevant robot dimensions based on the prototype shown in Fig. 1(b). (b) Parameters for bounds of an arbitrary deposition shape function.

Algorithm 2 Adaptive ramp building. Given a structure h_0, an initial position x_0, and a goal position x_*, the following algorithm builds a ramp over irregular structures based on local sensing. Assume, w.l.o.g. that $x_0 < x_*$.

1: **while** $x \neq x_*$ **do**
2: Move toward goal until $\exists y \in [x, x + r]$ that the pair y and $x + d$ violate condition (8) , or $x = x_*$
3: **if** $x \neq x_*$ **then**
4: Move to the lower point. (Note that all points in $[x_0, x + r)$ are climbable.)
5: Pick height according to Algorithm 1 and condition (12).
6: $x \leftarrow x - 2d$
7: **end if**
8: **end while**

By Theorem 4 the second term is bounded below by a positive number ε, thus

$$V(P[h_0], h_{n+1}) < V(P[h_0], h_n) - \varepsilon.$$

Since volume is always non-negative, condition (8) for making depositions must be violated after a finite number of steps N. □

4. Adaptive Ramp Building

The local deposition Algorithm 1 does not specify the points to be picked if the non-navigability condition (8) is true for multiple pairs, nor does it consider physical robot size or whether robots can reach deposition locations. The benefit of this vagueness is generality. Algorithm 1 works in arbitrary dimensions with an arbitrary number of robots making depositions in any order. It forms theoretical underpinning for Algorithm 2 (Fig. 3(b)), which takes such physical considerations into account. It gives a local deposition and motion strategy that allow robots in an arbitrary starting position $x_0 \in Q$ to reach a goal position $x_* \in Q$. By using a more or less conservative ϵ, the built structures can be made more or less smooth. While we focus on correctness, we point out some opportunities for improving efficiency.

4.1. Adaptive ramp building with a single robot

To solve the adaptive ramp building problem via Algorithm 1, robots need to identify point pairs that imply non-navigable features and make depositions. The strategy in Algorithm 2 is to move toward the goal x_* unless a robot encounters a non-navigable feature that impedes its progress. In that case, a robot deposits according to Algorithm 1 and backs up to check that the new deposition does not itself represent a non-navigable feature.

Since deposition and motion constraints depend on a robot's physical dimensions (Fig. 5(a)), additional parameter constraints are necessary to prove correctness of Algorithm 2. First, to guarantee that robots have enough room to back up, we assume that they start at a point $x_0 \in Q$ on the initial structure h_0 and can move freely within a radius of $r_0 \in \mathbb{R}^+$ without making any depositions,

$$P_K[h_0](y) = h_0(y), \quad \forall y \in B_{r_0}(x_0) \subset Q. \tag{10}$$

https://doi.org/10.1017/S0263574714000113 Published online by Cambridge University Press

Second, key dimensions of the robot as well as the deposition parameter K_D need to obey the following constraints (Fig. 5(a)):

$$K_D \geq K + \frac{\epsilon + l_{\text{height}}}{d}, \tag{11}$$

$$l_{\text{height}} > \epsilon, \tag{12}$$

$$r_0 > 2d + l_{\text{robot}}. \tag{13}$$

Condition (11) limits how far backward new depositions can extend into previously navigable terrain (Fig. 4(b)). It ensures that the motion and deposition strategy will not direct robots to deposit directly underneath themselves. Condition (12) ensures that the deposition mechanism has enough clearance to make depositions that conform with the assumptions in Algorithm 1. Condition (13), conservatively, ensures that a physical robot has enough space to back up.

Theorem 7. *Given a robot that fulfills parameter conditions (11)–(13) with starting position x_0 that fulfills (10) following Algorithm 2 will reach a goal point x_* after a finite number of steps.*

Proof. Denote the interval $[x_0 - r_0, x + d]$ in which no point pairs fulfill (8) by A (*accessible region*). Robots stay inside the accessible region at all times while finding points to deposit on. First, condition (12) guarantees that a robot can make a deposition of height ϵ, as required by Algorithm 1. Second, condition (11) guarantees that depositions with a maximum height of l_{height} made in the interval $[x, x + d]$ will not extend into $[x_0 - r_0, x - d]$. As a result, moving to $x - 2d$ after a deposition guarantees that no point pair in A fulfills (8). By (10) and the deposition strategy, there are always accessible points, i.e. $[x_0 - r_0, x_0] \subset A$. By Theorem 6 this algorithm terminates after a finite number of depositions with $x = x_*$. □

Figure 3(b) shows a series of depositions made via Algorithm 2. This strategy also guarantees that robots can always reach x_0 without requiring additional depositions, which could allow robots to replenish supplies. Conversely, the accessible region provides cooperating robots access to the deposition site, Section 4.2.

Physical depositions are not perfect cones (Fig. 1(b)). Algorithm 2 explicitly allows for uncertainty in the target structure (via ϵ), but not for deposition uncertainty. In fact, the upper bound for target structures requires that no depositions accidentally make intermediate structures larger than $P_K[h_0]$.

Following is a short description on how to address this problem and allow depositions with arbitrary continuous shape functions f (and bounded derivative $f'_{\max}$) as long as f can be sandwiched between two cones (Fig. 5(b)). As long as $l_{\text{dep}} < \epsilon$, Algorithm 1 (and as a result Algorithm 2) still works with the following substitutions: In Lemma 1 $f'_{\max}$ takes the place of K_D. In Theorem 4 the minimum height is $\epsilon - l_{\text{dep}}$ instead of ϵ. In Theorem 5 and condition (11) K_D is replaced with K_a. In addition to uncertainty in shape, this approach of bounding cones also allows for uncertainty in the exact deposition location and volume.

4.2. Adaptive ramp building with multiple robots

The locally reactive nature of Algorithm 2 makes extension to multiple robots easy. Robots do not need to communicate the state of the building process in order to cooperate. However, they still need to coordinate locally to determine which one deposits as to not obstruct one another. This section outlines two different approaches: first, cooperation to build large structures where each robot only has a limited amount of building material; second, cooperation to achieve speedup through parallelism when robots are initially distributed in the terrain.

Sensible strategies of what a robot should do after it runs out of building material depend on wether robots can move past one another. If they can, then multiple robots can cooperate by returning to the starting position and resupplying their stock of building material while other robots continue building. This approach takes advantage of the fact that Algorithm 2 maintains an accessible region A, which always allows robots to return to the starting position without having to make additional depositions.

A distributed implementation of this strategy that requires only local coordination between robots is shown in Fig. 6(a). It consists of three behavioral states. In *follow* mode a robot moves toward the

https://doi.org/10.1017/S0263574714000113 Published online by Cambridge University Press

Table I. Results of cooperative ramp building simulations with varying number of robots and deposition capacities. The table shows the 95% confidence intervals for estimating the mean number of simulation steps (5 samples). The speed of each robot is 0.05 per simulation step. Each deposition takes one simulation step. Reloading building supplies takes one simulation step. Variations in completion times arise from both additive noise to the deposition shape and random selection of deposition parameters from their legal ranges in Algorithm 1.

Capacity	1 Robot	2 Robots	3 Robots
5	1614 ± 82	869 ± 56	680 ± 40
10	1077 ± 39	577 ± 50	507 ± 31
20	719 ± 59	451 ± 31	436 ± 22

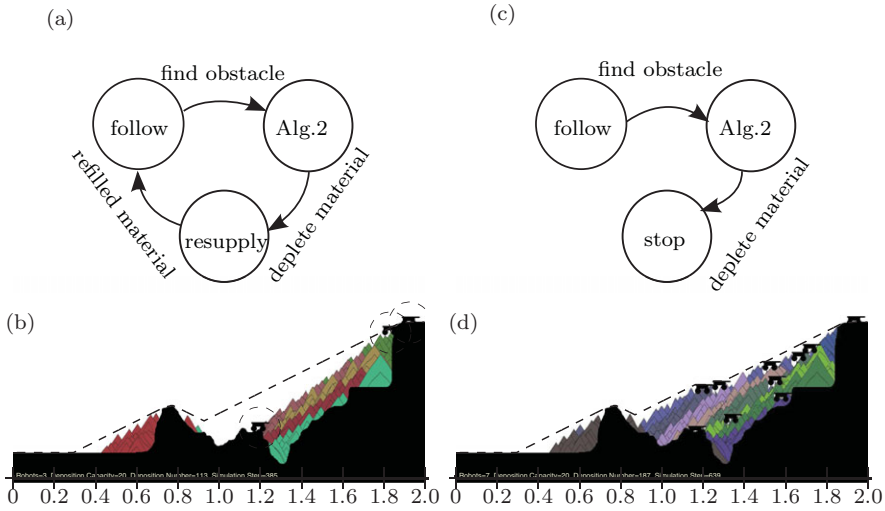

Fig. 6. (Colour online) Simulations of cooperative adaptive ramp building with limited building supplies. Parameters are $x_0 = 0.2$, $x_* = 1.9$, $d = 0.05$, and otherwise the same as in Fig. 3. (a) Behavioral state diagram for building when robots can pass one another, see text for state descriptions. (b) Final structure when three robots are limited to 20 depositions. Each deposition set is indicated by a different colour. (c) State diagram for building when robots cannot pass one another and, when depleted, become part of the ramp structure. (d) Simulation with 10 robots where each is limited to making 20 depositions, see simulation movies.[15]

goal and starts following any other robots that are not in resupply mode. When it senses an obstacle, it switches to executing Algorithm 2. Robots execute Algorithm 2 until they run out of building material and switch to a resupply mode. When a robot is in *resupply* mode, other robots cease following it and instead let the resupplying robot pass. The robot moves back toward the starting point where its stock of building material is restored. Once the resupply is finished, the robot switches back to follow mode.

Compared with a single robot resupplying this cooperative approach is faster because the team can keep building while individual robots resupply (Table I). The benefit of this strategy depends on the deposition capacity and the number of robots relative to the particular geometry of the problem. If the time it takes a robot to resupply and return to the building site is shorter than the time it takes all other robots to exhaust their building materials, there is no benefit to adding more robots to the team or expanding their capacity to carry building material, e.g. last line of Table I.

If robots cannot pass one another, the locally reactive nature of the algorithm can be used to treat spent robots as obstacles. The strategy is shown in Fig 6(c). Similar to the previous case, it consists of three behavioral states. The *follow* and ramp building modes are the same. Robots start in *follow* mode and execute it until they sense an obstacle. When a robot runs out of building material, it enters *stop*

https://doi.org/10.1017/S0263574714000113 Published online by Cambridge University Press

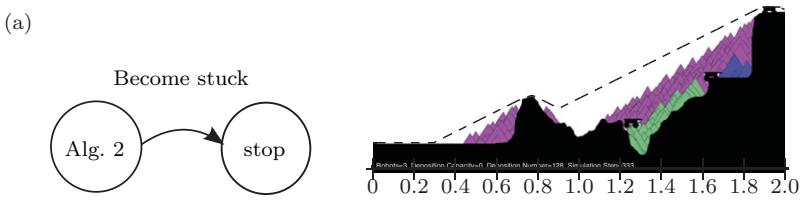

Fig. 7. (Colour online) Simulation of parallel adaptive ramp building. Parameters are the same as in Fig. 6. (a) Behavioral state diagram for parallel ramp building. Robots with unlimited supplies of building material execute Algorithm 2 until they become stuck. (b) Final structure (333 simulation steps) of multiple robots working concurrently. If a robot becomes stuck, it is treated as a obstacle by other robots.

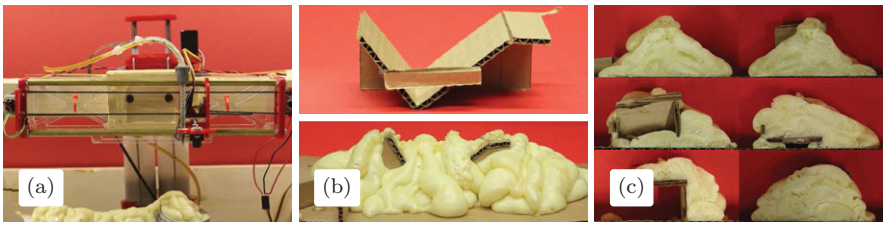

Fig. 8. (Colour online) Scanning foam deposition mechanism. (a) A scanning carriage holds a downward facing IR-distance sensor and mixing nozzle. Pressurized foam precursors are delivered to the nozzle by flexible tubing. (b) Top: Initial obstacle before leveling deposition; bottom: final structure after deposition episode. (c) Cross sections of final structure. Each leveling deposition episode represents one cone-like deposition in Algorithm 2.

mode, becomes inactive, and is treated as an obstacle by other robots (Fig. 6(d)). Strictly speaking, the correctness proof of Theorem 7 is no longer valid since robots cannot be resized like depositions, i.e. it is possible for a depleted robot to violate the upper bound constraint used in proving the stopping condition, Theorem 6. However, if a robot occasionally violates the upper bound, it simply creates a new one for subsequent depositions. As long as this bad behavior occurs rarely, one would expect Algorithm 2 to still yield correct results, e.g. Fig. 6(d). Investigating the exact conditions for termination with this execution model would be an interesting extension of this work. Alternatively, the depleted robot could make additional moves to optimize building progress or ensuring that it does not violate the invariant upper bound.

In the second scenario the starting positions of multiple robots are distributed along the construction path, e.g. dropped there to speed up construction, and each robot starts building a ramp via Algorithm 2. However, without initially fulfilling the starting condition (10) robots might become stuck, i.e. cannot move to an appropriate place to make the next deposition (Fig. 7(b) right). Further, without coordination one robot might deposit on another (Fig. 7(b) middle). Despite these failures, if one robot initially fulfills (10), the process will successfully complete. Other robots can provide speed up through parallelism until they become stuck. This approach is similar to Fig. 6(c) and illustrated in Fig. 7(a).

As the previous examples illustrate, the locally reactive nature of Algorithm 2 can be exploited to create distributed cooperative construction strategies for multiple robots. When structures are only modified by depositions, the proofs carry over directly. When defunct robots are treated as part of the structure, Algorithm 2 often works, but care must be taken to not repeatedly violate the upper bound $P_K[h_n]$.

4.3. Physical implementation and experimental results

We built a remote-controlled prototype robot (Fig. 1(b)) and a scanning foam deposition mechanism (Fig. 8(a)) for testing solutions to the key technical challenges presented by Algorithm 2. The prototype shows that robots can, in principle, build and navigate relatively large foam structures. The scanning deposition mechanism demonstrates autonomous leveling behavior that can be used to turn the physical construction problem into the simplified problem solved by Algorithm 2. The

https://doi.org/10.1017/S0263574714000113 Published online by Cambridge University Press

approach is to fix a path in the building domain and run the adaptive ramp building algorithm along this 1-dimensional subspace.

One major challenge is designing a deposition mechanism and selecting an appropriate material.[14] Both the prototype robot and scanning deposition mechanism use two compartment syringes with mixing nozzles (McMaster-Carr PN: 74695A11 with 74695A63, 7451A22 with 7816A32) and high expansion polyurethane casting foam (US-Composites 2 lb foam) to make amorphous depositions.

The scanning deposition mechanism consists of a mixing nozzle and distance sensor mounted on a moving carriage, Fig 8(a). By running Algorithm 1 along the direction of carriage travel (with $K = 0, \epsilon = 2$ cm and d covering all of Q), this mechanism autonomously creates a level structure from amorphous depositions. Mounting this mechanism on a robot and treating each leveling deposition episode as a single application of the deposition operator D, turns this physical construction task into the simplified problem solved by Algorithm 2. Viewed from the side, each leveled line under the carriage represents the apex of a conical deposition. Algorithm 2 simply picks the next point to level.

5. Conclusion

We developed a continuous model for amorphous depositions, and used it to prove correctness of a distributed algorithm that solves the adaptive ramp building problem. This example application illustrates how locally reactive behavior and amorphous building material together can create reliable building behavior in unstructured terrain.

Adaptive ramp building can also serve as a base behavior for composing more complicated behaviors. For example, it could guarantee accessibility to locations where support structures need to be built. With the ability to consistently encode virtual points in a group of robots, adaptive ramp building could be used to build arbitrary (K-Lipschitz) structures by building ramps to a carefully chosen set of virtual points: an approach we plan to explore.

There are a number of ways the presented algorithms could be improved. Our presentation focuses on correctness, not optimality. Robots could be much smarter about coordination between robots and deposition point selection to maximize the volume of each deposition, especially if their sensing radius was much larger than d. For implementations, it would also be worthwhile to explicitly consider different shape functions and structures that are not well modeled as functions, i.e. have overhangs.

6. Proofs

Proof. (Theorem 2) (1) Assume to the contrary that $\exists x, y \in Q$ s.t.

$$|P_K[h](x) - P[h](y)| > K|x - y|. \tag{14}$$

Assume w.l.o.g. that $P_K[h](y) \leq P_K[h](x)$ and since $P_K[h]$ is a positive scalar function, $|P_K[h](x) - P[h]_K(y)| = P_K[h](x) - P_K[h](y)$. Rearranging the terms in (14) leads to the contradiction $P_K[h](x) - K|x - y| > P_K[h](y)$, since the max in $P_K[h](y)$, see (7), is taken over the entire domain, including x. Therefore, points violating the Lipschitz condition cannot exist in $P[h]$. □

(2) Assume to the contrary that there exists a point $x \in Q$ s.t. $P_K[h](x) > g(x) \geq h(x)$. Since there cannot be equality between $P_K[h](x)$ and $g(x)$, the maximization in (7) must take its maximum value at some other point $y \in Q$. Rearranging $P_K[h](x) = h(y) - k|x - y| > g(x)$ results in $h(y) - g(x) > k|x - y|$, and since $g > h$ $g(y) - g(x) > k|x - y|$, which is a contradiction as it would violate the Lipschitz continuity of g. □

Proof. (Theorem 5) First, note that P can be applied to non-continuous functions, specifically continuous structures with a single discontinuous point. Let $\widetilde{h}_{n,(\phi,\sigma)}(x) = h_n(x) + (\sigma - h_n(\phi))\delta_\phi x$, where δ denotes the Kronecker delta, and σ and ϕ are selected according to Algorithm 1.

Next, since ϕ is in the search set of max for point $P_K[h_n](x)$ in (7), $h_n(\phi) \leq \sigma = h_n(\phi) + \omega \leq P_K[h_n](\phi)$, consequently

$$\widetilde{h}_{n,(\phi,\sigma)} \leq P_K[h_n]. \tag{15}$$

https://doi.org/10.1017/S0263574714000113 Published online by Cambridge University Press

Finally, since restricting $y \in \{x, \phi\} \subset Q$ in (7) results in the same expression as (2), thus $D[f_{(\phi,\sigma)}, h_n] = h_{n+1} \leq P_{K_D}[\widetilde{h}_{n,(\phi,\sigma)}]$.

By Theorem 3 and assuming that $K_D > K$, $P_{K_D}[\widetilde{h}_{n,(\phi,\sigma)}] \leq P_K[\widetilde{h}_{n,(\phi,\sigma)}]$. Together Theorem 2.2 and (15) imply that $P_K[\widetilde{h}_{n,(\phi,\sigma)}] \leq P_K[h_n]$, which results in the series of relations $h_{n+1} \leq P_K[\widetilde{h}_{n,(\phi,\sigma)}] \leq P_K[h_n]$. And again, by Theorem 2.2 $P_K[h_{n+1}] \leq P_K[h_n]$. However, $h_{n+1} \geq h_n$ implies $P_K[h_{n+1}] \geq P_K[h_n]$, thus $P_K[h_{n+1}] = P_K[h_n]$. By induction, $P_K[h_n] = P_K[h_0]$. □

Acknowledgments

This work was supported by the Wyss Institute for Biologically Inspired Engineering.

References

1. S. Berman, A. Halasz, M. A. Hsieh and V. Kumar, "Optimized stochastic policies for task allocation in swarms of robots," *IEEE Trans. Robot.* **25**(4) 927–937 (2009).
2. T. Bonwetsch, F. Gramazio and M. Kohler, "Digitally Fabricating Non-standardised Brick Walls," *ManuBuild*, Rotterdam, Netherlands (2007) pp. 191–196.
3. L. Brodbeck, L. Wang and F. Iida, "Robotic Body Extension Based on Hot Melt Adhesives," *Proceedings of IEEE International Conference on Robotics and Automation (ICRA)*, Saint Paul, MN (2012) pp. 4322–4327.
4. R. D'Andrea, "Flying machine enabled construction," available at: `http://www.idsc.ethz.ch/Research_DAndrea/Archives/Flying_Machine_Enabled_Construction` Accessed June 28, 2013.
5. K. C. Galloway, R. Jois and M. Yim, "Factory Floor: A Robotically Reconfigurable Construction Platform," *IEEE International Conference on Robotics and Automation (ICRA)* (May 2010) pp. 2467–2472.
6. A. Grushin and J. A. Reggia, "Automated design of distributed control rules for the self-assembly of pre-specified artificial structures," *Robot. Auton. Syst.* **56**(4), 334–359 (Apr. 2008).
7. D. Hjelle and H. Lipson, "A Robotically Reconfigurable Truss," *Proceedings of ASME/IFToMM International Conference on Reconfigurable Mechanisms and Robots* (Jun. 2009).
8. N. Khalili, *Emergency Sandbag Shelter: How to Build Your Own* (CalEarth Press, Hesperia, CA, 2008).
9. B. Khoshnevis, "Automated construction by contour crafting related robotics and information technologies," *J. Autom. Constr.* (Special Issue: The best of ISARC 2002) **13**, 5–19 (2004).
10. D. Ladley and S. Bullock, "Logistic Constraints on 3D Termite Construction," *Fourth International Workshop on Ant Colony Optimization and Swarm Intelligence* (2004) pp. 178–189.
11. Q. Lindsey, D. Mellinger and V. Kumar, "Construction of Cubic Structures with Quadrotor Teams," *Proceedings of Robotics: Science and Systems*, Los Angeles, CA (Jun. 2011). http://www.roboticsproceedings.org/rss07/p25.html.
12. S. Magnenat, R. Philippsen and F. Mondada, "Autonomous construction using scarce resources in unknown environments," *Auton. Robots* **33**, 467–485 (2012).
13. N. Napp and E. Klavins, "A compositional framework for programming stochastically interacting robots," *Int. J. Robot. Res.* **30**(6), 713–729 (2011).
14. N. Napp, O. Rappoli, J. Wu and R. Nagpal, "Materials and Mechanisms for Amorphous Robotic Construction," *Proceedings of IEEE/RSJ International Conference on Intelligent Robots and Systems (IROS)* (2012) pp. 4879–4885.
15. N. Napp and R. Nagpal, "Simulation videos of adaptive ramp construction," available at: `http://www.eecs.harvard.edu/ssr/movies/amorphous-construction/`. Accessed June 28, 2013.
16. A. W. Naylor and G. R. Sell, *Linear Opearator Theory in Engineering and Science*, Applied Mathematical Sicences (Springer, New York, NY, 1982).
17. K. Petersen, R. Nagpal and J. Werfel, "Termes: An Autonomous Robotic System for Three-Dimensional Collective Construction," *Proceedings of Robotics: Science and Systems*, Los Angeles, CA (Jun. 2011). http://www.roboticsproceedings.org/rss07/p35.html.
18. S. Revzen, M. Bhoite, A. Macasieb and M. Yim, "Structure Synthesis On-the-Fly in a Modular Robot," *Proceedings of IEEE/RSJ Conference on Intelligent Robots and Systems (IROS)* (2011) pp. 4797–4802.
19. G. Theraulaz and E. Bonabeau, "Coordination in distributed building," *Science* **269**(5224) 686–688 (1995).
20. J. S. Turner, *The Externded Organism. The Physiology of Animal-Built Structures* (Harvard University Press, Cambridge, MA, 2004).
21. US Army Corps of Engineers Northwestern Division, *Sandbagging Techniques* (US Army. Corps of Engineers. Northwestern Division, Portland, OR, 2004).
22. J. Werfel and R. Nagpal, "Three-dimensional construction with mobile robots and modular blocks," *Int. J. Rob. Res.* **27**, 463–479 (Mar. 2008).